Localization induced by pressure in pyrochlore $Bi_2Ir_2O_7$

Wei Liu,[1,2] Hui Han,[1,2] Langsheng Ling,[1] Long Ma,[1] Li Pi,[1,3] Lei Zhang,[1,*] and Yuheng Zhang[1,3]

[1] *Anhui Key Laboratory of Condensed Matter Physics at Extreme Conditions, High Magnetic Field Laboratory, Chinese Academy of Sciences, Hefei 230031, China*

[2] *University of Science and Technology of China, Hefei 230026, China*

[3] *Hefei National Laboratory for Physical Sciences at the Microscale, University of Science and Technology of China, Hefei 230026, China*

(Dated: September 7, 2017)

Abstract

In this work, the resistivity and magnetization of $Bi_2Ir_2O_7$ are investigated under hydrostatic pressure. At ambient pressure, the resistivity of $Bi_2Ir_2O_7$ exhibits a metallic behavior with the decrease of temperature. When the pressure is applied, a metal-insulator phase transition at low temperature is induced under a pressure of ~ 0.48 GPa. The metal-insulator phase transition temperature (T_{MI}) increases linearly with pressure as $\mathrm{d}T_{MI}/\mathrm{d}P = 3.4 \pm 0.3$ K/GPa. The temperature dependence of resistivity [$\rho(T)$] in the pressure-induced insulating phase exhibits a thermal activation behavior ($\rho = \rho_0 e^{\Delta E/k_B T}$), where the thermal activation energy (ΔE) increases monotonously with the pressure. Meanwhile, the magnetization is enhanced by the pressure, which indicates an enhancement of magnetic ordering. The results suggest that localization occurs due to the magnetic ordering induced by the pressure, which confirms the magneto-electronic coupling in $Bi_2Ir_2O_7$

PACS numbers: 71.30.+h, 61.50.Ks, 74.62.Fj

Keywords: pyrochlore $Bi_2Ir_2O_7$; pressure effect; metal-insulator phase transition; localization

*Corresponding author. Email:zhanglei@hmfl.ac.cn

I. INTRODUCTION

Recently, the pyrochlore iridates $A_2Ir_2O_7$ (A = lanthanide, yttrium, or bismuth) have been paid significant attention due to the prominent physical phenomena rang form spin liquid states, spin ice, field-induced spin quantum transition, to possible topological non-trivial state [1–9]. These exotic phenomena originate from the multiple interplays involving spin, orbit, charge, and lattice degrees of freedom, such as the effective spin $J = 1/2$ magnetic moments of Ir-5d electrons caused by the strong spin-orbital coupling, the geometrical frustration produced by the corner-sharing tetrahedra, the large crystal field resulted from the octahedron [9, 10]. The cell of pyrochlore $A_2Ir_2O_7$ is cubic structure belonging to $Fd\bar{3}m$ space group [11], the structure of which is usually described as two interpenetrating networks of A_2O, and BO_6, whose vertices are occupied by spins leading to strong geometrical frustration [12, 13]. As we know, the iridium-based pyrochlore oxides are prototypical materials with more extended $5d$ orbits, which prone to form much strong spin-orbital coupling compared with those in $3d$ transition-metal oxides [10]. The strong spin-orbital coupling and electron-lattice coupling rise the orbital degeneracy and narrow the bandwidths of $5d$ orbits, which lead iridium-based systems near a bandwidth-controlled metal-insulator transition (MIT) [10, 14]. Actually, most of $A_2Ir_2O_7$ oxides undergo an MIT except $Pr_2Ir_2O_7$ and $Bi_2Ir_2O_7$ which keep paramagnetic metallic behavior down to low temperature [8, 15, 16]. Moreover, the MIT occurs concomitantly with a transition to an all-in/all-out (AIAO) magnetic ordering state [5, 17].

In the pyrochlore oxides, $Bi_2Ir_2O_7$ is special and prominent due to its metallic behavior down to very low temperature and lack of long-range magnetic ordering [18, 19]. The Bi^{3+} ions on A-sites are biggest among the $A_2Ir_2O_7$ compounds. However, its lattice lies between that of $Eu_2Ir_2O_7$ and $Nd_2Ir_2O_7$. Recent study on $Bi_2Ir_2O_7$ uncovers unconventional physical properties at very low temperature [16]. Moreover, the muon spin relaxation (μSR) reveals two weak magnetic transitions at 1.84 K and 0.23 K respectively at low temperature, which shows up an exotic ground state in $Bi_2Ir_2O_7$ [19].

Although many studies on this compound, the nature of the transport and weak magnetic properties in $Bi_2Ir_2O_7$ are still not completely clarified. A bandwidth-controlled MIT is expected despite of metallic behavior in $Bi_2Ir_2O_7$. As we know, the hydrostatic pressure is a pure method to drive more dramatic changes in various physical parameters, such as electron

correlations, magnetic interactions, and bandwidths [20–23]. In this work, the resistivity and magnetization of $Bi_2Ir_2O_7$ are investigated under hydrostatic pressure. When a pressure is applied, an insulating phase at low temperature is induced under a pressure of $\sim$ 0.48 GPa. The transition temperature (T_{MI}) increases linearly with pressure as $dT_{MI}/dP = 3.4$ $\pm$0.3 K/GPa. Moreover, the magnetization is increased by the pressure, which suggests the enhancement of magnetic ordering induces the MIT in $Bi_2Ir_2O_7$.

II. EXPERIMENT

A polycrystalline sample of $Bi_2Ir_2O_7$ was synthesized by the solid-state reaction method. The starting materials, powders of Bi_2O_3 (purity 99.9 %) and IrO_2 (99.99 %) were mixed thoroughly according to the stoichiometric ratio of 1 : 2. The mixed powders were sintered at 1173 K for 4 days with several intermediate grindings. The structure and phase purity were checked by the Rigaku-TTR 3 X-ray diffractometer with high-intensity graphite monochromatized Cu Kα radiation. The resistivity measurements were performed using the conventional four-probe method with the temperature varied using a closed-cycle helium refrigeration unit. The DC magnetization was measured by a Magnetic Property Measurement System (Quantum Design MPMS 7 T-XL) with a superconductive quantum interference device (SQUID). The hydrostatic high-pressure was realized by using a clamp-type piston pressure cell, where Daphne 7373 oil was employed as the medium to transmit pressure with a high level of high homogeneity. To calibrate the pressures at room temperature, we used Cu_2O powder as a manometer, whose nuclear quadrupole resonance frequency as a function of pressure has been determined very accurately [24].

III. RESULTS AND DISCUSSION

Figure 1 depicts the temperature dependence of resistivity [$\rho(T)$] for $Bi_2Ir_2O_7$ under selected pressures up to 2.24 GPa, where the inset shows that under ambient pressure on log-log scale. As we know, physical behaviors of $A_2Ir_2O_7$ systems correlate closely with the ionic radius of A^{3+} ions, which influences the bandwidth of Ir-5d band by changing the Ir-O-Ir bond angle [4, 14, 22]. The ionic radius of Bi^{3+} (1.17 Å) is the biggest compared with the lanthanide or yttrium among $A_2Ir_2O_7$ systems [25]. However, $Bi_2Ir_2O_7$ lies between $Eu_2Ir_2O_7$

and $Nd_2Ir_2O_7$ in terms of its lattice constant [26]. Moreover, the $6p$ orbit of Bi^{3+} situates at near the Fermi level and hybridizes strongly with the Ir-$5d$ bands, which expands the $5d$ bandwidth of Ir^{4+} [27]. Therefore, a metallic behavior is expected for $Bi_2Ir_2O_7$ [27, 28]. Under ambient pressure as given in the inset of Fig. 1, the $\rho(T)$ curve of $Bi_2Ir_2O_7$ indeed exhibits a metallic behavior with $d\rho/dT > 0$ in the whole measurement temperature range, which is in agreement with the theoretic prediction and previous reports [16, 18].

It is well know that the electronic correlation in $A_2Ir_2O_7$ can be manipulated by ionic radius on A-sites through the modulation of bond length and bond angle [14]. Actually, it has been demonstrated that the modulation of A-ions by chemical doping of Y or Ca does induce phase transitions at low temperature in $Bi_2Ir_2O_7$ [29, 30]. However, the chemical doping inevitably brings in disorders and defects, which will significantly affect the transport behavior in the system. On the other hand, the hydrostatic pressure is known as a pure device compared with the chemical doping, which can effectively modulate electron correlations, magnetic interactions, and bandwidths. In addition, it has been demonstrated that pressure below $\sim$ 2.4 GPa does not destroy the lattice symmetry of $A_2Ir_2O_7$ [20]. Thus, the change of properties below $\sim$ 2.4 GPa is only caused by the change of bond length and bond angle. In view of this, hydrostatic pressures up to 2.24 GPa are applied to $Bi_2Ir_2O_7$. When the pressure is applied, all $\rho(T)$ curves under different pressures for $Bi_2Ir_2O_7$ exhibit similar behaviors, as shown in the main panel of Fig. 1. However, in addition to the raise and lowering of $\rho(T)$ curves by the pressure, tiny changes occurs to $\rho(T)$ curves, especially in low temperature range.

In order to clearly clarified the influence of pressure on the resistivity of $Bi_2Ir_2O_7$, the $\rho(T)$ curves in low temperature range below 30 K are magnified, as shown in Fig. 2 (a). Under ambient pressure, the $\rho(T)$ presents a metallic behavior down to 4 K, except a tiny rise at low temperature. In fact, study shows that $Bi_2Ir_2O_7$ exhibits a metallic behavior down to 2 K without any phase transition [19]. When the pressure is applied, changes happen to the $\rho(T)$ curve. As shown in Fig. 2 (a), the $\rho(T)$ curve under $P = 0.16$ GPa still keeps a metallic behavior down to 4 K, which is analogy to that under ambient pressure. However, the a upturn occurs to $\rho(T)$ curve under $P = 0.48$ GPa, where the slope of $\rho(T)$ changes from positive ($d\rho/dT > 0$) to negative ($d\rho/dT < 0$) with the decrease of temperature. As the pressure further increases, the region of $d\rho/dT < 0$ expands. Generally, positive $d\rho/dT$ suggests a metallic behavior, while negative $d\rho/dT$ indicates an insulating one [22].

Therefore, the change of $d\rho/dT$ form positive to negative induced by the pressure gives a clue of a pressure-induced MIT.

The MIT temperature (T_{MI}) can be quantified by the minimum point of $\rho(T)$, as indicated by the triangles in Fig. 2 (a). Figure 3 (a) plots the T_{MI} vs. P extracted from Fig. 2 (a). As can be seen, the MIT appears above $P \sim 0.48$ GPa. The T_{MI} depends linearly on the pressure up to 2.24 GPa. As mentioned above, pressure below ~ 2.4 GPa does not destroy the lattice symmetry of $A_2Ir_2O_7$ [20]. Thus, the linear dependence of T_{MI} on P confirms that the pressure has linear effect on the transport properties of $Bi_2Ir_2O_7$. The linear fitting of T_{MI} vs. P gives that $dT_{MI}/dP = 3.4 \pm 0.3$ GPa/K and the intercept $I = 7.7 \pm 0.4$ K. The increase of T_{MI} with the increase of P suggests a positive pressure effect. In fact, in the $A_2Ir_2O_7$ system, $Gd_2Ir_2O_7$ and $Eu_2Ir_2O_7$ also exhibit positive pressure effects with $dT_{MI}/dP = 6.2 \pm 0.4$ GPa/K and 3.5 ± 0.2 GPa/K respectively [31]. In contrary, $Sm_2Ir_2O_7$ displays a negative pressure effect with $dT_{MI}/dP = -13.2 \pm 0.8$ GPa/K [31]. In addition, $Nd_2Ir_2O_7$ present a negative pressure effect [23]. Thus, it can be seen that pressure effects in $A_2Ir_2O_7$ exhibit various tendencies, which indicates complex correlation and interactions in these systems.

Generally, for the gapped insulating system, its resistivity usually follows the thermally activated exponential behavior called Arrhenius's law:

$$\rho = \rho_0 e^{\Delta E/k_B T} \tag{1}$$

Where ρ_0 represents the residual resistivity, ΔE is the activation energy, and k_B is the Boltzmann constant. According to the Arrhenius's law, the $\ln\rho$ depends linearly on T^{-1}. Figure 2 (b) gives the $\ln\rho$ vs. T^{-1} at low temperatures under different pressures. It can be seen that the $\ln\rho$ vs. T^{-1} at low temperatures under different pressures exhibits a linear relation except those under $P = 0$ and 0.16 GPa. The linear behavior of $\ln\rho$ vs. T^{-1} unambiguously suggests a gapped insulating behavior. The linear fitting of $\ln\rho$ vs. T^{-1} is performed, where ΔE as a function of P is plotted in Fig. 3 (b). It can be seen that ΔE increases monotonously as the pressure increases.

As we know, the MIT in $A_2Ir_2O_7$ usually occurs concomitantly with the spin ordering transition of an all-in/all-out spin configuration, which suggests a coupling between electron and magnetism [3, 7]. Thus, the magnetization of $Bi_2Ir_2O_7$ under pressures should be investigated to clarify the relation between the transport and magnetism. Figure 4 shows the

field dependence of magnetization [$M(H)$] under ambient pressure at selected temperature. It can be seen that all $M(H)$ curves exhibit paramagnetic behaviors without long-range spin-ordering, which is in agreement with the previous reports [16, 30]. However, it has been demonstrated that $Bi_2Ir_2O_7$ exhibits weak ferromagnetic behavior at very low temperature [19].

Figure 5 (a) shows the $M(H)$ curves at 4 K under selected pressures. At the fixed pressure, the magnetization increases as the pressure increases, which indicates that the magnetic ordering tendency becomes more and more prominent. This result suggests that the pressure enhances the magnetic coupling in this system. Figure 5 (b) gives the saturation magnetization [M_S] at 7 T as a function of pressure. The M_S increases monotonously with the increase of pressure, which indicates the enhancement of the magnetization by the pressure.

These results suggest that the MIT induced by the pressure is correlated with the enhancement of magnetization by the pressure, which indicates intimate magneto-electronic coupling in this system. In fact, an MIT is also induced by the Ca-doping on A-sites in $Bi_{2-x}Ca_xIr_2O_7$ [30]. However, the substitution of Bi^{3+} by Ca^{2+} brings holes, defects, disorders in the system in addition to the change of bond length and bond angle. In this work, through the pressure which is a pure device, it is demonstrated that an MIT can be induced by the pressure. In fact, the pressure brings two effects into the system, the shrinkage of the bond length and the change of the bond angle. As we know, the ionic radius of Bi^{3+} is bigger than any other in $A_2Ir_2O_7$. However, its lattice constant lies between that of $Eu_2Ir_2O_7$ and $Nd_2Ir_2O_7$. Both $Eu_2Ir_2O_7$ and $Nd_2Ir_2O_7$ undergo an MIT with the decrease of temperature. If speculated from the aspect of bond length, the $Bi_2Ir_2O_7$ should also undergo an MIT. Instead, $Bi_2Ir_2O_7$ exhibits a metallic behavior in the whole measuring temperature range, which suggests the bond length is not determinant fact in the MIT. It is noticed that the bond angle of $Bi_2Ir_2O_7$ is close to those of $Nd_2Ir_2O_7$, $Sm_2Ir_2O_7$, and $Eu_2Ir_2O_7$, all of which undergo MITs [26]. On the other hand, it has been demonstrated that the pressure tends to change the Ir-O-Ir bond angle by rotating the IrO_6 octahedron in the iridates [32]. Therefore, in the $A_2Ir_2O_7$, the change of bond angle by pressure tends to play a determinant role in the transport behavior. The experimental results of pressure suggest that the decrease of Ir-O-Ir bond angle in $Bi_2Ir_2O_7$ enhances magnetic ordering, which in turn leads to the localization of the itinerant electrons.

IV. CONCLUSION

In summary, the resistivity and magnetization of $Bi_2Ir_2O_7$ are investigated under hydrostatic pressure. An MIT at low temperature is induced on the $\rho(T)$ by the pressure of $\sim$ 0.48 GPa. The T_{MI} increases linearly with pressure as $\mathrm{d}T_{MI}/\mathrm{d}P = 3.4 \pm 0.3$ K/GPa, which shows a positive pressure effect. The magnetization is enhanced by the pressure, which indicates an enhancement of magnetic ordering. The results suggest that the itinerant electrons are localized due to the magnetic ordering induced by the pressure, which confirms the magneto-electronic coupling in $Bi_2Ir_2O_7$.

V. ACKNOWLEDGEMENTS

This work is supported by the National Key R&D Program of China (Grant Nos. 2017YFA0303201 and 2016YFA0401003) and the National Natural Science Foundation of China (Grant Nos. 11574322, U1332140, U1732276, and 11574288).

[1] Y. Machida, S. Nakatsuji, S. Onoda, T. Tayama, T. Sakakibara, Time-reversal symmetry breaking and spontaneous Hall effect without magnetic dipole order, Nature **463** 210 (2010).

[2] E. Ma, Y. Cui, K. Ueda, S. Tang, K. Chen, N. Tamura, P. Wu, J. Fujioka, Y. Tokura, and Z. Shen, Mobile metallic domain walls in an all-in-all-out magnetic insulator, Science **350** (2015) 538.

[3] Z. Tian, Y. Kohama, T. Tomita, H. Ishizuka, T. Hsieh, J. Ishikawa, K. Kindo, L. Balents, and S. Nakatsuji, Field-induced quantum metal-insulator transition in the pyrochlore iridate $Nd_2Ir_2O_7$, Nat. Phys. **12** (2015) 134.

[4] M. Nakayama, Takeshi Kondo, Z. Tian, J. J. Ishikawa, M. Halim, C. Bareille, W. Malaeb, K. Kuroda, T. Tomita, S. Ideta, K. Tanaka, M. Matsunami, S. Kimura, N. Inami, K. Ono, H. Kumigashira, L. Balents, S. Nakatsuji, and S. Shin, Slater to Mott Crossover in the Metal to Insulator Transition of $Nd_2Ir_2O_7$, Phy. Rev. Lett. **117** (2016) 056403.

[5] C. Donnerer, M. C. Rahn, M. Moretti Sala, J. G. Vale, D. Pincini, J. Strempfer, M. Krisch, D. Prabhakaran, A. T. Boothroyd, and D. F. McMorrow, All-in-all-Out Magnetic Order and Propagating Spin Waves in $Sm_2Ir_2O_7$, Phys. Rev. Lett. **117** (2016) 037201.

[6] K. Ueda, J. Fujioka, B. J. Yang, J. Shiogai, A. Tsukazaki, S. Nakamura, S. Awaji, N. Nagaosa, and Y. Tokura, Magnetic Field-Induced Insulator-Semimetal Transition in a Pyrochlore $Nd_2Ir_2O_7$, Phys. Rev. Lett. **115** (2015) 056402.

[7] H. Shinaoka, S. Hoshino, M. Troyer, and P. Werner, hase Diagram of Pyrochlore Iridates: All-in-All-out Magnetic Ordering and Non-Fermi-Liquid Properties, Phys. Rev. Lett. **115** (2015) 156401.

[8] S. Nakatsuji, Y. Machida, Y. Maeno, T. Tayama, T. Sakakibara, J. V. Duijn, L. Balicas, J. N. Millican, R. T. Macaluso, and J. Y. Chan, Metallic Spin-Liquid Behavior of the Geometrically Frustrated Kondo Lattice $Pr_2Ir_2O_7$, Phys. Rev. Lett. **96** (2006) 087204.

[9] D. Pesin and L. Balents, Mott physics and band topology in materials with strong spin-orbit interaction, Nat. Phys. **6** (2010) 376.

[10] B. J. Kim, H. Jin, S. J. Moon, J. Y. Kim, B. G. Park, C. S. Leem, J. Yu, T. W. Noh, C. Kim, S. J. Oh, J. H. Park, V. Durairaj, G. Cao, and E. Rotenberg, Novel Jeff = 1/2 Mott State Induced by Relativistic Spin-Orbit Coupling in Sr_2IrO_4. Phys. Rev. Lett. **101** (2008) 076402.

[11] J. Gardner, M. Gingras, and J. Greedan, Magnetic pyrochlore oxides, Rev. Mod. Phys. **82** (2010) 53.

[12] M. A. Subramanian, G. Aravamudan, and G. V. S. Rao, Oxide Pyrochlores − A Review, Prog. Solid State Chem. **15** (1983) 55.

[13] R. L. Withers, T. R. Welberry, A. K. Larsson, Y. Liu, L. Noren, H. Rundlof, and F. J. Brink, Local crystal chemistry, induced strain and short range order in the cubic pyrochlore $(Bi_{1.5-\alpha}Zn_{0.5-\beta})(Zn_{0.5-\gamma}Nb_{1.5-\delta})O_{(7-1.5\alpha-\beta-\gamma-2.5\delta)}$ (BZN), J. Solid State Chem. **177** (2004) 231.

[14] K. Matsuhira, M .Wakeshima, R. Nakanishi, Y. Yamada, A. Nakamura, W. Kawano, S. Takagi, and Y. Hinatsu, Metal-Insulator Transitions in Pyrochlore Oxides $Ln_2Ir_2O_7$, J. Phys. Soc. Jpn. **76** (2007) 043706.

[15] R. J. Bouchard and J. L. Gillson, New Family Of Bismuth − Precious Metal Pyrochlores, Mat. Res. Bull. **6** (1971) 669.

[16] T. F. Qi, O. B. Korneta, X. G. Wan, L. E. DeLong, P. Schlottmann, and G. Cao, Strong magnetic instability in correlated metallic $Bi_2Ir_2O_7$, J. Phys.: Condens. Matter **24** (2012) 345601.

[17] X. G. Wan, A. M. Turner, A. Vishwanath, and S. Y. Savrasov, Topological semimetal and

Fermi-arc surface states in the electronic structure of pyrchlore iridates, Phys. Rev. B **83** (2011) 205101.

[18] Y. S. Lee, S. J. Moon, Scott C. Riggs, M. C. Shapiro, I. R. Fisher, Bradford W. Fulfer, Julia Y. Chan, A. F. Kemper, and D. N. Basov, Infrared study of the electronic structure of the metallic pyrochlore iridate $Bi_2Ir_2O_7$, Phys. Rev. B **87** (2013) 195143.

[19] P. J. Baker, J. S. Moller, F. L. Pratt, W. Hayes, S. J. Blundell, T. Lancaster, T. F. Qi, and G. Cao, Weak magnetic transitions in pyrochlore $Bi_2Ir_2O_7$, Phys. Rev. B **87** (2013) 180409(R).

[20] G. Prando, R. Dally, W. Schottenhame Z. Guguchia, S. H. Baek, R. Aeschlimann, A. U. B. Wolter, S. D. Wilson, B. Buchner, and M. J. Graf, Influence of hydrostatic pressure on the bulk magnetic properties of $Eu_2Ir_2O_7$, Phys. Rev. B **93** (2016) 104422.

[21] K. Ueda, J. Fujioka, C. Terakura, and Y. Tokura, Pressure and magnetic field effects on metal-insulator transitions of bulk and domain wall states in pyrochlore iridates, Phys. Rev. B **92** (2015) 121110(R).

[22] F. F. Tafti, J. J. Ishikawa, A. McCollam, S. Nakatsuji, and S. R. Julian, Pressure-tuned insulator to metal transition in $Eu_2Ir_2O_7$, Phys. Rev. B **85** (2012) 205104.

[23] M. Sakata, T. Kagayama, K. Shimizu, K. Matsuhira, S. Takagi, M. Wakeshima, and Y, Hinatsu, Suppression of metal-insulator transition at high pressure and pressure-induced magnetic ordering in pyrochlore oxide $Nd_2Ir_2O_7$, Phys. Rev. B **83** (2011) 041102(R).

[24] A. P. Reyes, E. T. Ahrens, R. H. Heffner, P. C. Hammel, and J. D. Thompson, Cuprous oxide manometer for high-pressure magnetic resonance experiments, Rev. Sci. Instrum. **63** (1992) 3120.

[25] R. D. Shannon, Revised Effective Ionic Radii and Systematic Studies of Interatomie Distances in Halides and Chaleogenides, Acta Cryst. **A32** (1976) 751.

[26] H. B. Zhang, K. Haule, and D. Vanderbilt, Metal-Insulator Transition and Topological Properties of Pyrochlore Iridates, Phys. Rev. Lett. **118** (2017) 026404.

[27] B. B. Hinojosa, J. C. Nino, and A. Asthagiri, First-principles study of cubic Bi pyrochlores, Phys. Rev. B **77** (2008) 104123.

[28] Q. Wang, Y. Cao, X. G. Wan, J. D. Denlinger, T. F. Qi, O. B. Korneta, G. Cao, and D. S. Dessau, Experimental electronic structure of the metallic pyrochlore iridate $Bi_2Ir_2O_7$, J. Phys.: Condens. Matter **27** (2015) 015502.

[29] N. Aito, M. Soda, Y. Kobayashi, and M. Sato, Spin-Glass-like Transition and Hall Resistivity

of $Y_{2-x}Bi_xIr_2O_7$, J. Phys. Soc. Jpn. **72** (2003) 1226.

[30] D. D. Liang, H. Liu, N. Liu, L. S. Ling, Y. Y. Han, L. Zhang, C. J. Zhang, Structural, magnetic and electrical properties in the pyrochlore oxide $Bi_{2-x}Ca_xIr_2O_{7-\delta}$, Cer. Int. **42** (2016) 4562.

[31] W. Liu, H. Han, L. Ma, L. Pi, L. Zhang, and Yuheng Zhang, Different pressure effects in $A_2Ir_2O_7$ (A = Gd, Eu, and Sm), unpublished.

[32] Y. Ding, L. Yang, C. Chen, H. Kim, M. Han, W. Luo, Z. Feng, M. Upton, D. Casa, J. Kim, T. Gog, Z. Zeng, G. Cao, H. Mao, and M. Veenendaa, Pressure-Induced Confined Metal from the Mott Insulator $Sr_3Ir_2O_7$, Phys. Rev. Lett. **116** (2016) 216402.

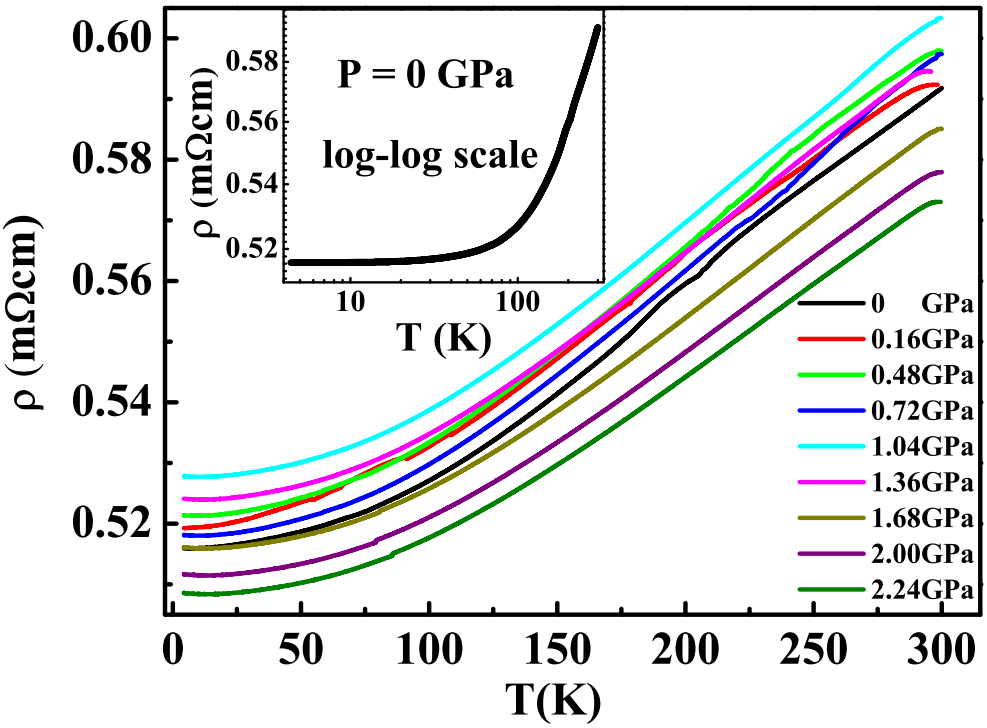

FIG. 1: (Color online) Temperature dependence of resistivity [$\rho(T)$] under selected pressures for $Bi_2Ir_2O_7$ [the inset shows the $\rho(T)$ curve under ambient pressure on log-log scale].

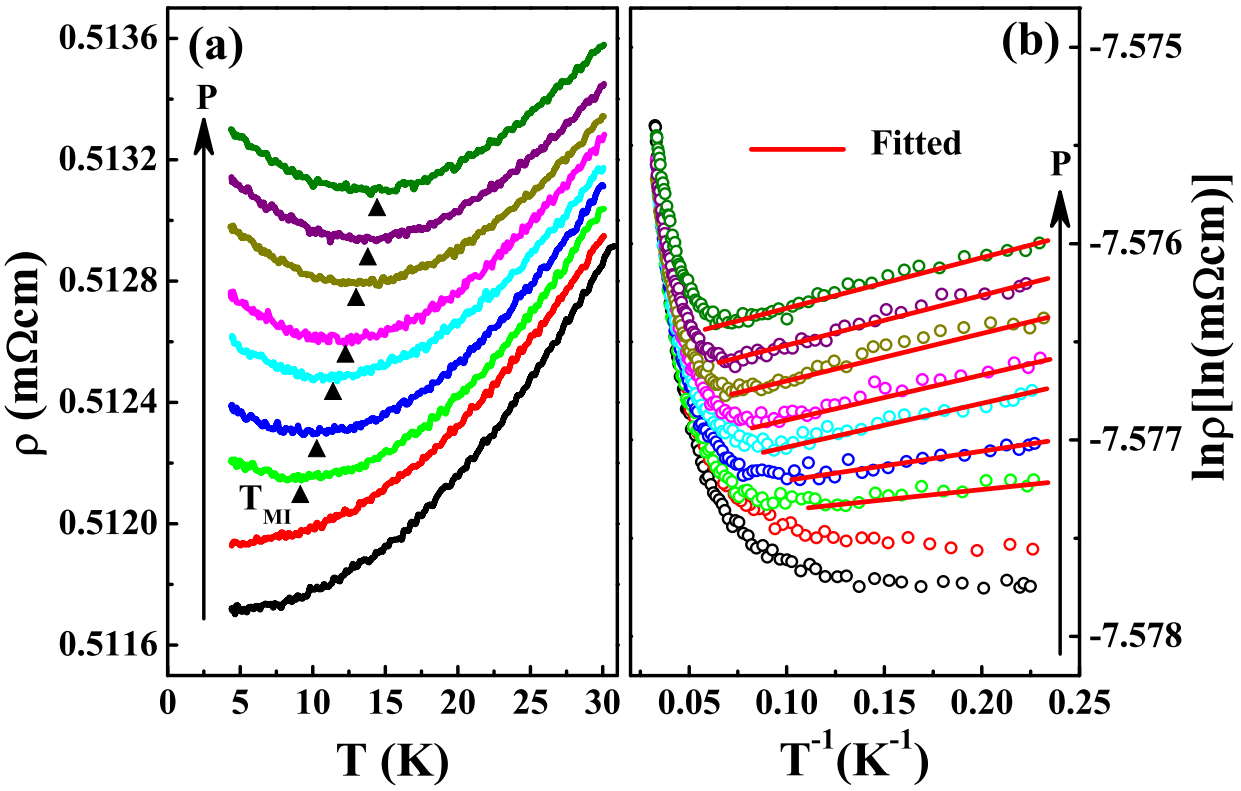

FIG. 2: (Color online) (a) The $\rho(T)$ curves in low temperature region below 30 K under different pressures for $Bi_2Ir_2O_7$; (b) the lnρ vs. T^{-1} curves with the fitted lines under different pressures [the $\rho(T)$ curves are moved vertically for clear clarity except that under ambient pressure].

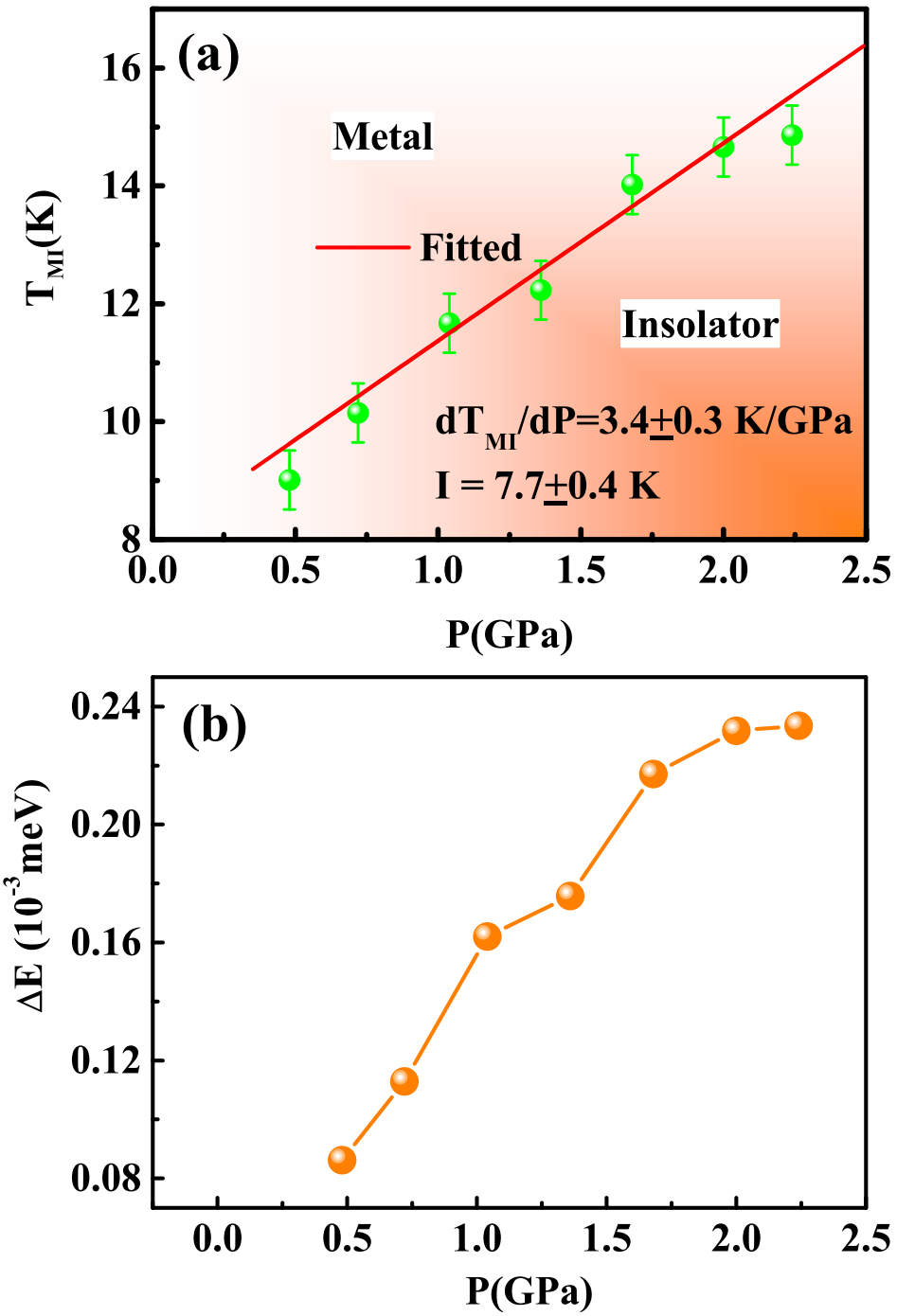

FIG. 3: (Color online) (a) The transition temperature T_{MI} as a function of pressure (P) for $Bi_2Ir_2O_7$ (the line is fitted); (b) the activation energy ΔE as a function of P.

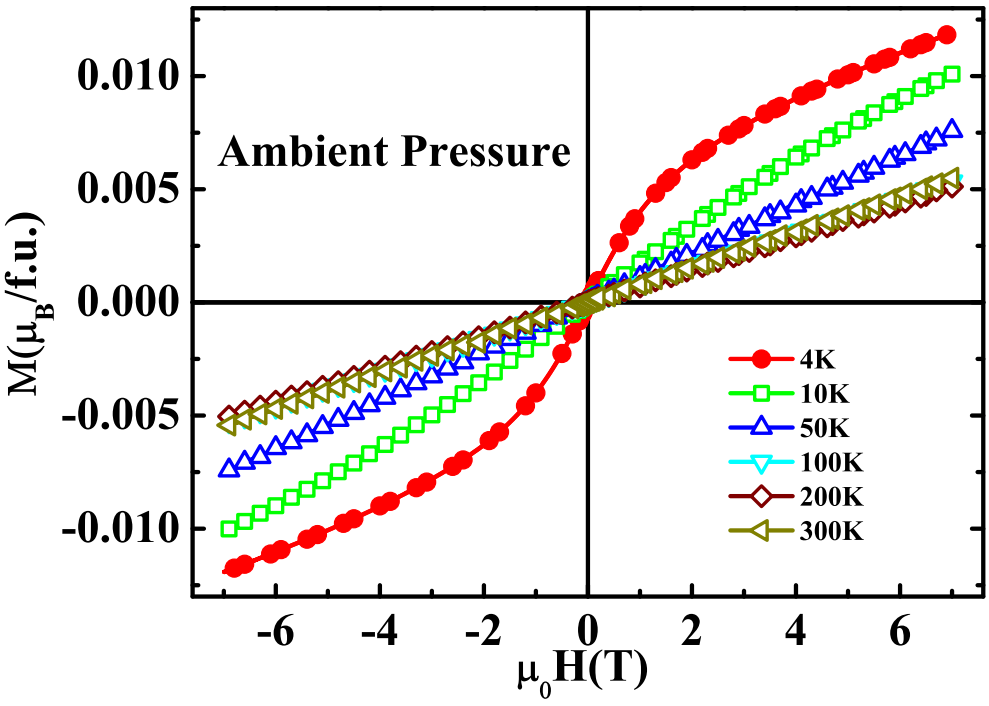

FIG. 4: (Color online) The field dependence of magnetization $[M(H)]$ at selected temperatures.

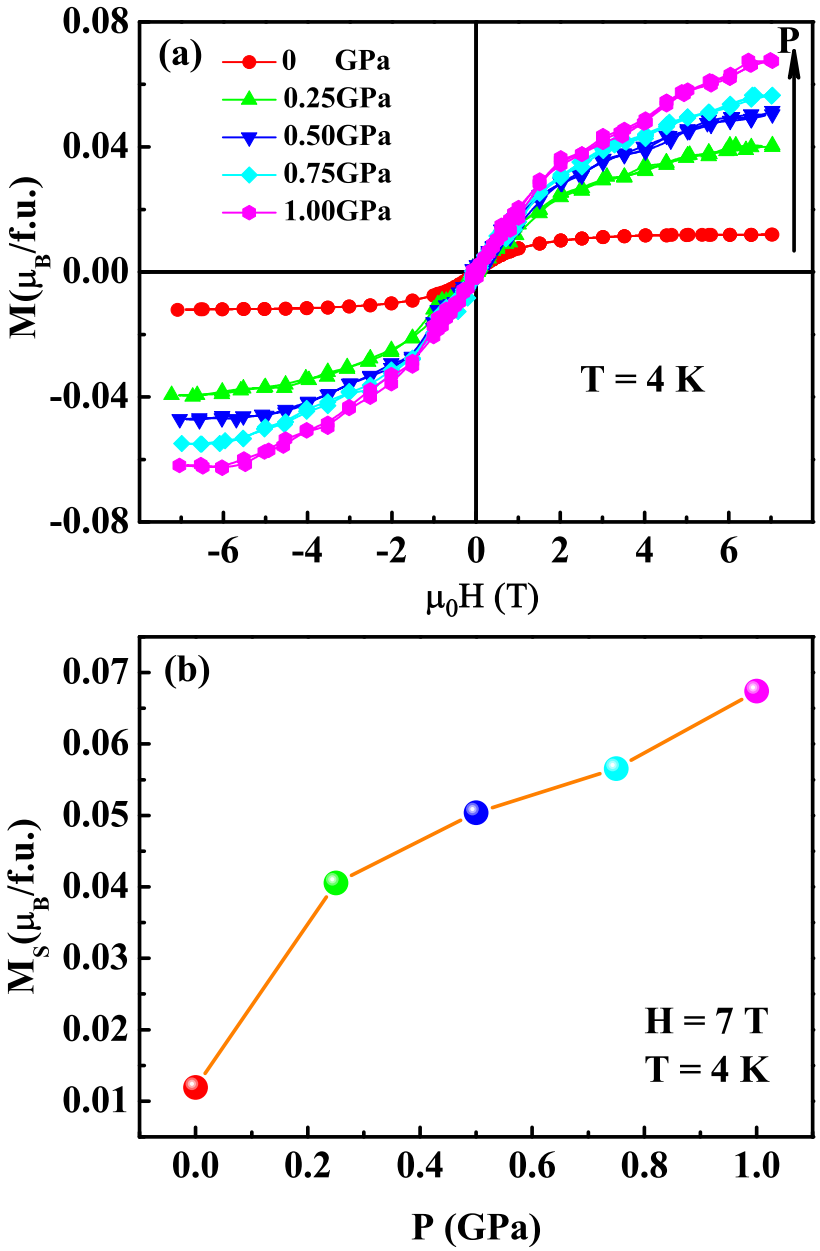

FIG. 5: (Color online) (a) The $M(H)$ under selected pressures at $T = 4$ K; (b) the saturation magnetization (M_S) as a function P.